

Link-Layer Capacity of Downlink NOMA with Generalized Selection Combining Receivers

Vaibhav Kumar*, Barry Cardiff*, Shankar Prakriya†, and Mark F. Flanagan*

*School of Electrical and Electronic Engineering, University College Dublin, Belfield, Dublin 4, Ireland

†Department of Electrical Engineering, Indian Institute of Technology – Delhi, New Delhi, India

Email: vaibhav.kumar@ucdconnect.ie, barry.cardiff@ucd.ie, shankar@ee.iitd.ernet.in, mark.flanagan@ieee.org

Abstract—Non-orthogonal multiple access (NOMA) has drawn tremendous attention, being a potential candidate for the spectrum access technology for the fifth-generation (5G) and beyond 5G (B5G) wireless communications standards. Most research related to NOMA focuses on the system performance from Shannon’s capacity perspective, which, although a critical system design criterion, fails to quantify the effect of delay constraints imposed by future wireless applications. In this paper, we analyze the performance of a single-input multiple-output (SIMO) two-user downlink NOMA system, in terms of the link-layer achievable rate, known as effective capacity (EC), which captures the performance of the system under a delay-limited quality-of-service (QoS) constraint. For signal combining at the receiver side, we use generalized selection combining (GSC), which bridges the performance gap between the two conventional diversity combining schemes, namely selection combining (SC) and maximal-ratio combining (MRC). We also derive two approximate expressions for the EC of NOMA-GSC which are accurate at low-SNR and at high-SNR, respectively. The analysis reveals a tradeoff between the number of implemented receiver radio-frequency (RF) chains and the achieved performance, and can be used to determine the appropriate number of paths to combine in a practical receiver design.

Index Terms—non-orthogonal multiple access, effective capacity, generalized selection combining

I. INTRODUCTION

Worldwide efforts to enable 5G and B5G wireless communications are well underway, including new spectrum allocation policies, flexible modulation techniques, multiple-access schemes, standardization, and implementation. NOMA has received tremendous attention as a design paradigm for the radio access techniques of future communications standards due to its inherent potential for higher spectral efficiency, denser connectivity and lower latency [1]. In contrast to the traditional *orthogonal* radio-access schemes, multiple users in NOMA are served in the same resource block (time slot, subcarrier, frequency band, or spreading code). It was shown in [2] that when the channels from the source to each of the multiple

users are significantly different, NOMA can achieve a higher spectral efficiency as compared to its orthogonal multiple access (OMA) counterpart. In order to further enhance the spectral efficiency, different advanced signal processing schemes have been suggested, including cooperative NOMA [3], multi-antenna-assisted architectures for NOMA [4] and multiple-input multiple-output NOMA (MIMO-NOMA) [5]. Most existing research related to the performance analysis of NOMA systems has dealt primarily with the metrics of outage probability, achievable rate and system throughput.

Although the classical (Shannon) ergodic capacity has been extremely successful in communication system design, it fails to explicitly characterize the delay-constrained performance, which is one of the most crucial system design parameters for 5G and B5G networks. To facilitate the investigation of wireless networks under statistical QoS limitations (e.g., data rate, delay and delay-violation probability), a link-layer analysis tool, known as *effective capacity*, was first introduced in [6]. Given a delay-violation probability, the EC defines the maximum data arrival rate that can be supported by a radio link. The EC analysis of a multiple-input single-output (MISO) system in Nakagami- m , Rician and generalized- \mathcal{K} fading was presented in [7]. Recently, the EC analysis of a MISO system under the Fisher-Snedecor \mathcal{F} fading was presented in [8].

The available literature on the performance analysis of NOMA in terms of EC is relatively limited. In [9], the achievable link-layer rate of a multi-user downlink NOMA network under a per-user delay QoS requirement was presented, where the users were divided into multiple NOMA pairs and OMA was applied for multiple access among each such NOMA pair. It was shown that in such a scenario, OMA outperforms NOMA in terms of the total link-layer rate in the low signal-to-noise-ratio (SNR) regime, while at high SNR, the NOMA system achieves higher EC as compared to its OMA-based counterpart. It was shown in [10] that for a two-user downlink NOMA system, the optimal power control problem to maximize the sum effective capacity is non-convex and thus the notion of *partial effective capacity* was introduced to derive a sub-optimal power allocation policy. For the case of half/full-duplex two-user cooperative NOMA, in order to

This publication has emanated from research conducted with the financial support of Science Foundation Ireland (SFI) and is co-funded under the European Regional Development Fund under Grant Number 13/RC/2077.

maximize the minimum effective capacity of the user-pair, a bisection-based optimal power allocation scheme was proposed in [11]. Analysis of the delay-violation probability and EC for a multi-user downlink NOMA system using stochastic network calculus (SNC) was presented in [12]. The analysis of *effective secrecy rate* for a multi-user downlink NOMA system was recently presented in [13].

In all of the aforementioned research related to the EC analysis of NOMA, a single-input single-output (SISO) system model was considered. In this paper, we consider a single-input multiple-output (SIMO) downlink NOMA system consisting of two users¹. Although MRC is an optimal receiver combining technique for a SIMO system, it is highly susceptible to channel estimation error for the paths having lower instantaneous received SNR. On the other hand, SC uses the best path (in terms of SNR) and hence fails to exploit the total diversity offered by the other independent paths. A comparatively more flexible diversity combining scheme, called GSC, bridges this gap between SC and MRC, by adaptively combining a subset of the strongest paths. Therefore, GSC receivers are more robust to channel estimation errors and also require fewer active RF chains at the receiver, thereby reducing the overall cost of the system implementation. A detailed moment generating function (MGF)-based performance analysis of GSC in Rayleigh fading channels, in terms of bit error rate (BER), symbol error rate (SER) and outage probability, was presented in [14]. The performance analysis of GSC in a downlink NOMA system in terms of average achievable sum-rate and outage probability was presented in [15].

Against this background, the main contributions in this paper are listed below:

- We analyze the sum effective capacity of a two-user downlink NOMA system with GSC receivers. For the case of the symbol intended for the strong user, we derive an exact closed-form expression for the EC. On the other hand, for the case of the symbol intended for the weak user, since it is somewhat tedious to find an exact closed-form expression for the EC in NOMA-GSC, we derive closed-form expressions for two special cases, namely NOMA-SC and NOMA-MRC. We also show that most of the gain (in terms of sum EC) is achieved by combining the strongest diversity paths, and that diminishing returns are obtained as the number of combined paths increases.
- We derive low-SNR as well as high-SNR approximations for the sum EC of NOMA-GSC. From the analysis of the EC for the symbol intended for the weak user, it can be noted that no significant benefit of multiple receive antennas is observed at the weak user. Also, the results indicate that the

¹Note that a two-user downlink version of NOMA, called *multiuser superposition transmission* (MUST), has been proposed for the Third Generation Partnership Project Long Term Evolution Advanced (3GPP-LTE-A) standard.

sum EC grows exponentially with SNR in the low-SNR regime, and linearly with SNR in the high-SNR regime.

- Using Jensen's inequality, we derive a fundamental upper-bound on the sum EC of NOMA-GSC which is independent of the delay constraint. We show that this bound is equal to the average achievable sum rate of NOMA-GSC and that the difference between the achievable sum rate and the sum EC increases with increasing SNR and with an increase in the delay exponent.
- For the purpose of comparison, we also derive a closed-form expression for the sum EC of a two-user downlink OMA-GSC system, and show that NOMA-GSC outperforms OMA-GSC in terms of sum EC for any number of combined paths. We show that as the delay constraint becomes more strict, the performance difference between NOMA-GSC and OMA-GSC becomes smaller.

II. SYSTEM MODEL

Consider the two-user downlink NOMA system consisting of a source S equipped with a single transmit antenna, and two users U_s (the user with *strong* channel conditions) and U_w (the user with *weak* channel conditions) equipped with $N_s \geq 1$ and $N_w \geq 1$ receive antennas, respectively. We assume a half-duplex communication protocol. The channel coefficients between S and U_s are assumed to be independent and identically distributed (i.i.d.) according to $\mathcal{CN}(0, \Omega_s)$ with mean-square value Ω_s , while those between S and U_w are assumed to be i.i.d. according to $\mathcal{CN}(0, \Omega_w)$ with mean-square value equal to Ω_w . We assume that $\Omega_w < \Omega_s$, and that for each link perfect CSI is available at the receiver side, whereas only the knowledge of Ω_s and Ω_w is available at the transmitter side².

The source transmits a power-domain multiplexed symbol $\sqrt{a_s \mathcal{E}} x_s + \sqrt{a_w \mathcal{E}} x_w$ to both users, where $x_i, i \in \{s, w\}$ denotes the information-bearing constellation symbol intended for user U_i (here we assume that $\mathbb{E}\{|x_i|^2\} = 1$), \mathcal{E} is the energy budget at the source for each time slot, a_i is the power allocation coefficient with $a_s < a_w$ and $\sum_i a_i = 1$. Upon signal reception, user U_s (resp. U_w) adaptively selects a subset of $n_s, 1 \leq n_s \leq N_s$ (resp. $n_w, 1 \leq n_w \leq N_w$) antennas, out of the total N_s (resp. N_w) antennas which provide the strongest links (in terms of the received SNR), and then applies MRC to combine the received signals. Therefore, the signals received at user U_i (after applying GSC) is given by

$$\mathbf{y}_i = \mathbf{h}_i^H \left[\mathbf{h}_i \left(\sqrt{a_s \mathcal{E}} x_s + \sqrt{a_w \mathcal{E}} x_w \right) + \mathbf{z}_i \right],$$

²This is different from the two-user NOMA system presented in [9], where (perfect) *instantaneous* CSI was assumed to be available at the transmitter and therefore the users were ordered instantaneously (in terms of strong and weak users). In our system, the users are ordered depending on the *statistical* CSI. This reduces the signaling overhead at the transmitter and the overall system implementation cost.

where $\mathbf{h}_i = [h_{i,1} h_{i,2} \dots, h_{i,n_i}]^T \in \mathbb{C}^{n_i \times 1}$ contains the n_i largest-magnitude channel coefficients between S and U_i in *decreasing* order, i.e., $|h_{i,1}| \geq |h_{i,2}| \geq \dots \geq |h_{i,n_i}|$, and $\mathbf{z}_i = [z_{i,1} z_{i,2} \dots, z_{i,n_i}]^T \in \mathbb{C}^{n_i \times 1}$. Each element in \mathbf{z}_i represents additive white Gaussian noise (AWGN) with zero mean and variance σ^2 .

Both U_s and U_w first decode x_w considering the interference from x_s as additional noise. User U_s then applies successive interference cancellation (SIC) to decode the intended symbol x_s . Since the symbol x_w needs to be decoded correctly at both users (at U_w as the intended symbol and at U_s for SIC), while x_s needs to be correctly decoded only at user U_s , the received instantaneous SINR and SNR for the correct decoding of x_w and x_s are, respectively, given by

$$\gamma_w = \frac{a_w g_{\min} \rho}{a_s g_{\min} \rho + 1}, \quad \gamma_s = a_s g_s \rho,$$

where $g_i \triangleq \mathbf{h}_i^H \mathbf{h}_i$, $g_{\min} \triangleq \min\{g_s, g_w\}$ and $\rho \triangleq \mathcal{E}/\sigma^2$. Using a transformation of random variables and [14, eqn. (16)], the probability density function (PDF) of g_i can be given by

$$f_{g_i}(x) = \binom{N_i}{n_i} \left[\frac{x^{n_i-1} \exp\left(\frac{-x}{\Omega_i}\right)}{\Omega_i^{n_i} (n_i-1)!} + \frac{1}{\Omega_i} \sum_{l=1}^{N_i-n_i} (-1)^{n_i+l-1} \times \binom{N_s-n_s}{l} \binom{n_i}{l}^{n_i-1} \exp\left(\frac{-x}{\Omega_i}\right) \left\{ \exp\left(\frac{-lx}{n_i \Omega_i}\right) - \sum_{m=0}^{n_i-2} \frac{1}{m!} \left(\frac{-lx}{n_i \Omega_i}\right)^m \right\} \right]. \quad (1)$$

III. PERFORMANCE ANALYSIS

In this section, we present a comprehensive performance analysis of the two-user NOMA-GSC system in terms of effective capacity. We also derive closed-form approximations to the sum EC of NOMA-GSC, which are valid in the low-SNR and high-SNR regimes respectively, as well as an upper-bound on the sum EC. For a fair comparison, we also present the sum EC analysis of an OMA-GSC system.

A. Effective capacity of NOMA-GSC

The expression for EC of symbol x_i in NOMA-GSC can be given by (c.f. [9])

$$E_i = -\frac{1}{\theta T B} \ln [\mathbb{E} \{ \exp(-\theta T B R_i) \}], \quad (2)$$

where θ is the delay QoS exponent (denotes the asymptotic delay-rate of the buffer occupancy at the transmitter, defined as $\theta \triangleq -\lim_{x \rightarrow \infty} \ln \Pr\{L > x\}/x$, L being the equilibrium queue-length of the buffer at the transmitter), T is the length of each fading-block (this is assumed to be same for all the wireless links and an integer multiple of the symbol duration³), B is the total available bandwidth, and R_i is the instantaneous achievable rate for symbol

³We also assume that the symbol durations for both x_s and x_w are the same.

x_i (defined as $R_i = \log_2\{1 + \gamma_i\}$). It is important to note that $\theta \rightarrow \infty$ represents a system with very stringent delay constraint, while $\theta \rightarrow 0$ corresponds to the system with no delay constraint. For the case when $\theta \rightarrow 0$, the effective capacity becomes equal to the average achievable rate. Substituting the expression for the instantaneous achievable rate into (2), the expression for the effective capacity of symbol x_i in NOMA-GSC can be given by

$$E_i = -\frac{1}{\nu} \log_2 \left[\mathbb{E}_{\gamma_i} \left\{ (1 + \gamma_i)^{-\nu} \right\} \right], \quad (3)$$

where $\nu \triangleq \theta T B / \ln 2$. Therefore, for x_s , we have

$$E_s = -\frac{1}{\nu} \log_2 \left[\int_0^\infty (1+x)^{-\nu} f_{\gamma_s}(x) dx \right]. \quad (4)$$

Substituting the expression for $f_{g_s}(x)$ from (1) into (4), a closed-form expression for E_s can be given by

$$E_s = -\frac{1}{\nu} \log_2 \left[\binom{N_s}{n_s} \left\{ \frac{I_1}{\Omega_s^{n_s} (n_s-1)!} + \frac{1}{\Omega_s} \sum_{l=1}^{N_s-n_s} (-1)^{n_s+l-1} \times \binom{N_s-n_s}{l} \binom{n_s}{l}^{n_s-1} \left\{ I_2(l) - \sum_{m=0}^{n_s-2} \frac{I_3(m)}{m!} \left(\frac{-l}{n_s \Omega_s}\right)^m \right\} \right\} \right], \quad (5)$$

where $I_1 \triangleq \int_0^\infty (1 + a_s \rho x)^{-\nu} x^{n_s-1} \exp\left(\frac{-x}{\Omega_s}\right) dx = \frac{1}{\Gamma(\nu)} \int_0^\infty x^{n_s-1} G_{1,1}^{1,1} (a_s \rho x \mid 1-\nu) G_{0,1}^{1,0} \left(\frac{x}{\Omega_s} \mid -\right) dx = \frac{1}{\Gamma(\nu)(a_s \rho)^{n_s}} G_{1,2}^{2,1} \left(\frac{1}{\Omega_s a_s \rho} \mid 0, \nu-n_s\right)$, $I_2(l) \triangleq \int_0^\infty (1 + a_s \rho x)^{-\nu} \exp\left[\frac{-1}{\Omega_s} \left(1 + \frac{l}{n_s}\right) x\right] dx = \frac{\Phi_{s,l}^{\nu-1}}{(a_s \rho)^\nu} \exp(\Phi_{s,l}/a_s \rho) \Gamma(1-\nu, \Phi_{s,l}/a_s \rho)$ and $I_3(m) \triangleq \int_0^\infty (1 + a_s \rho x)^{-\nu} \exp(-x/\Omega_s) x^m dx = \frac{1}{\Gamma(\nu)(a_s \rho)^{m+1}} G_{1,2}^{2,1} \left(\frac{1}{\Omega_s a_s \rho} \mid 0, \nu-m-1\right)$. Here $G_{\cdot,\cdot}^{a,\cdot}(\cdot)$ denotes Meijer's G-function, $\Gamma(\cdot, \cdot)$ represents the upper-incomplete Gamma function and $\Phi_{s,l} \triangleq (1 + \frac{l}{n_s})/\Omega_s$. The integration in I_1 is solved using [16, eqns. (7), (10), (11), (21) and (22)], the integration in $I_2(l)$ is solved using [17, eqn. (3.382-4), p. 347], and the integration in $I_3(m)$ is solved similarly to I_1 .

On the other hand, using (3), the EC for x_w can be given by

$$E_w = -\frac{1}{\nu} \log_2 \left[\int_0^\infty \left(1 + \frac{a_w \rho x}{a_s \rho x + 1}\right)^{-\nu} f_{g_{\min}}(x) dx \right]. \quad (6)$$

The PDF of g_{\min} can be given by $f_{g_{\min}}(x) = f_{g_w}(x)[1 - F_{g_s}(x)] + f_{g_s}(x)[1 - F_{g_w}(x)]$. It can be noted that the expression for the PDF of g_{\min} is very complicated and hence deriving an exact closed-form expression for E_w is somewhat tedious. Therefore, we discuss two special cases for the EC of x_w .

Case I ($n_s = n_w = n = 1$): In this case, the NOMA-GSC system reduces to the NOMA-SC system where the signal from a single path (which has the highest instantaneous received SINR) is selected at both U_s and U_w . Defining $g_{\min,SC} \triangleq \min\{|h_{s,1}|^2, |h_{w,1}|^2\}$, using a transformation of random variables, it can be shown that $f_{g_{\min,SC}}(x) = \sum_{k=1}^{N_s} \sum_{j=1}^{N_w} (-1)^{k+j} \binom{N_s}{k} \binom{N_w}{j} \chi_{k,j} \exp(-\chi_{k,j}x)$, where $\chi_{k,j} \triangleq \frac{k}{\Omega_s} + \frac{j}{\Omega_w}$. Therefore, replacing $f_{g_{\min}}(x)$ in (6) by $f_{g_{\min,SC}}(x)$, a closed-form expression for the EC of x_w in a NOMA-GSC system with $n = 1$ can be given by

$$E_{w,SC} = \frac{-1}{\nu} \log_2 \left[\frac{1}{\Gamma(\nu)\Gamma(-\nu)} \sum_{k=1}^{N_s} \sum_{j=1}^{N_w} (-1)^{k+j} \binom{N_s}{k} \binom{N_w}{j} \frac{\chi_{k,j}}{\rho} \mathcal{G}_{1,1:1,1:1,0}^{1,1:1,1:1,0} \left(\begin{matrix} 0 \\ \nu-1 \end{matrix} \middle| \begin{matrix} 1+\nu \\ 0 \end{matrix} \middle| \begin{matrix} - \\ 0 \end{matrix} \middle| a_s, \frac{\chi_{k,j}}{\rho} \right) \right],$$

where $\mathcal{G}_{1,1:1,1:1,0}^{1,1:1,1:1,0}(\cdot)$ denotes the extended generalized bivariate Meijer G-function (EGBMGF) and the integral is solved using [16, eqns. (10), (11)] and [18, eqn. (9)].

Case II ($n_s = N_s, n_w = N_w$): In this case, the NOMA-GSC system reduces to the NOMA-MRC system where signals from all the diversity paths are combined. Defining $g_{\min,MRC} \triangleq \min_{i \in \{s,w\}} \left\{ \sum_{n=1}^{N_i} |h_{i,n}|^2 \right\}$, using a transformation of random variables it can be shown that $f_{g_{\min,MRC}}(x) = \frac{x^{N_s-1}}{\Gamma(N_s)\Omega_s^{N_s}} \exp(-\chi_{1,1}x) \sum_{j=0}^{N_w-1} \frac{x^j}{j!\Omega_w^j} + \frac{x^{N_w-1}}{\Gamma(N_w)\Omega_w^{N_w}} \exp(-\chi_{1,1}x) \sum_{k=0}^{N_s-1} \frac{x^k}{k!\Omega_s^k}$. Therefore, replacing $f_{g_{\min}}(x)$ in (6) by $f_{g_{\min,MRC}}(x)$, a closed-form expression for the EC of x_w in a NOMA-GSC system with $n_s = N_s$ and $n_w = N_w$ can be given by

$$E_{w,MRC} = \frac{-1}{\nu} \log_2 \left[\frac{1}{\Gamma(N_s)\Omega_s^{N_s}} \sum_{j=0}^{N_w-1} \frac{\rho^{-(N_s+j)}}{j!\Omega_w^j} \times \mathcal{G}_{1,1:1,1:1,0}^{1,1:1,1:1,0} \left(\begin{matrix} 1-(N_s+j) \\ \nu-(N_s+j) \end{matrix} \middle| \begin{matrix} 1+\nu \\ 0 \end{matrix} \middle| \begin{matrix} - \\ 0 \end{matrix} \middle| a_s, \frac{\chi_{k,j}}{\rho} \right) + \frac{1}{\Gamma(N_w)\Omega_w^{N_w}} \times \sum_{k=0}^{N_s-1} \frac{\rho^{-(N_w+k)}}{k!\Omega_s^k} \mathcal{G}_{1,1:1,1:1,0}^{1,1:1,1:1,0} \left(\begin{matrix} 1-(N_w+k) \\ \nu-(N_w+k) \end{matrix} \middle| \begin{matrix} 1+\nu \\ 0 \end{matrix} \middle| \begin{matrix} - \\ 0 \end{matrix} \middle| a_s, \frac{\chi_{k,j}}{\rho} \right) \right].$$

The sum effective capacity for NOMA-GSC is then obtained as $E_{\text{sum}} = E_s + E_w$.

B. Effective capacity of OMA-GSC

For a fair comparison, we also present a closed-form analysis for the EC of OMA-GSC in this subsection. Considering a time-division multiplexed system, S transmits $\sqrt{\mathcal{E}}x_w$ and $\sqrt{\mathcal{E}}x_s$ in the first and second time slots, respectively. The instantaneous achievable rate for x_i is given by $\hat{R}_i = 0.5 \log_2(1 + \hat{\gamma}_i)$, where $\hat{\gamma}_i = \rho g_i$. Therefore, similar to (3), the EC of x_i for OMA-GSC can be given by

$$\begin{aligned} \hat{E}_i &= -\frac{1}{\nu} \log_2 \left[\mathbb{E}_{\hat{\gamma}_i} \left\{ (1 + \hat{\gamma}_i)^{-\nu/2} \right\} \right] \\ &= -\frac{1}{\nu} \log_2 \left[\int_0^\infty (1 + \rho x)^{-\nu/2} f_{g_i}(x) dx \right]. \end{aligned} \quad (7)$$

Substituting the expression for $f_{g_i}(x)$ from (1) into (7), a closed-form expression for \hat{E}_i is given by

$$\begin{aligned} \hat{E}_i &= \frac{-1}{\nu} \log_2 \left[\binom{N_i}{n_i} \left\{ \frac{\hat{I}_{i,1}}{\Omega_i^{n_i} (n_i - 1)!} + \frac{1}{\Omega_i} \sum_{l=1}^{N_i - n_i} (-1)^{n_i + l - 1} \right. \right. \\ &\quad \left. \left. \times \binom{N_i - n_i}{l} \binom{n_i}{l}^{n_i - 1} \left\{ \hat{I}_{i,2}(l) - \sum_{m=0}^{n_i - 2} \frac{\hat{I}_{i,3}(m)}{m!} \left(\frac{-l}{n_i \Omega_i} \right)^m \right\} \right\} \right], \end{aligned} \quad (8)$$

where $\hat{I}_{i,1} \triangleq \int_0^\infty (1 + \rho g_i)^{-\nu/2} x^{n_i - 1} \exp(-x/\Omega_i) dx = \frac{1}{\Gamma(\nu/2)\rho^{n_i}} G_{1,2}^{2,1} \left(\frac{1}{\Omega_i \rho} \middle| \begin{matrix} 1 - n_i \\ 0, \frac{\nu}{2} - n_i \end{matrix} \right)$, $\hat{I}_{i,2}(l) \triangleq \int_0^\infty (1 + \rho x)^{-\nu/2} \exp(-\Phi_{i,l}x) dx = \left(\Phi_{i,l}^{(\nu/2)-1} / \rho^{\nu/2} \right) \exp(\Phi_{i,l}/\rho) \Gamma(1 - \frac{\nu}{2}, \Phi_{i,l}/\rho)$, and $\hat{I}_{i,3}(m) \triangleq \int_0^\infty (1 + \rho x)^{-\nu/2} x^m \exp(-x/\Omega_i) dx = \frac{1}{\Gamma(\nu/2)\rho^{m+1}} G_{1,2}^{2,1} \left(\frac{1}{\Omega_i \rho} \middle| \begin{matrix} -m \\ 0, \frac{\nu}{2} - m - 1 \end{matrix} \right)$. The integrals in $\hat{I}_{i,1}$, $\hat{I}_{i,2}(l)$ and $\hat{I}_{i,3}(m)$ are solved similar to I_1 , $I_2(l)$ and $I_3(m)$ respectively. The sum effective capacity for OMA-GSC is then obtained by $\hat{E}_{\text{sum}} = \hat{E}_w + \hat{E}_s$.

C. High-SNR approximation for the EC of NOMA-GSC

In this subsection, we present a high-SNR approximation for the EC of NOMA-GSC. For $\rho \gg 1$, it can be noted from (3) that, for x_s , we have

$$\begin{aligned} E_s &\approx -\frac{1}{\nu} \log_2 \left[\mathbb{E}_{g_s} \left\{ (a_s \rho g_s)^{-\nu} \right\} \right] \\ &= \log_2(a_s \rho) - \frac{1}{\nu} \log_2 \left[\int_0^\infty x^{-\nu} f_{g_s}(x) dx \right] \\ &= \log_2(a_s \rho) - \frac{1}{\nu} \log_2 \left[\binom{N_s}{n_s} \left(\frac{\Gamma(n_s - \nu)}{\Omega_s^\nu \Gamma(n_s)} + \frac{1}{\Omega_s} \sum_{l=1}^{N_s - n_s} (-1)^{n_s + l - 1} \binom{N_s - n_s}{l} \binom{n_s}{l}^{n_s - 1} \left\{ \Gamma(1 - \nu) \Phi_{s,l}^{\nu-1} \right. \right. \right. \\ &\quad \left. \left. \left. - \sum_{m=0}^{n_s - 2} \frac{\Gamma(m - \nu + 1) \Omega_s^{m - \nu + 1}}{m!} \left(\frac{-l}{n_s \Omega_s} \right)^m \right\} \right\} \right], \end{aligned} \quad (9)$$

where the integral is solved using [17, eqn. (3.351-3), p. 340] and the integral holds good for $\nu < \min\{n_s, 1, m + 1\} = 1$. A similar limitation was encountered in the analysis in [7]. On the other hand, for the case of x_w , a high-SNR approximation for the EC of x_w can be given by

$$E_w \approx \log_2 \left(1 + \frac{a_w}{a_s} \right). \quad (10)$$

It is interesting to note from (10) that at high SNR, the effective capacity of x_w is independent of θ and N_w . This means that at high SNR, the EC of x_w becomes (almost) equal to the average achievable rate of x_w and no gain is obtained (in terms of the EC of x_w) by having multiple antennas at U_w . For $\rho \gg 1$, an approximation for the sum EC can be obtained by adding (9) and (10).

D. Low-SNR approximation for the EC of NOMA-GSC

A low-SNR ($\rho \rightarrow 0$) approximation for the EC can be given by (c.f. [7, eqn. (18)])

$$\dot{E}_i = \rho \dot{\tilde{E}}_i + 0.5\rho^2 \ddot{\tilde{E}}_i + O(\rho^2), \quad (11)$$

where $\dot{\tilde{E}}_i$ and $\ddot{\tilde{E}}_i$ denote the first and second order derivatives of the EC in (3) with respect to ρ and evaluated at $\rho = 0$, and $O(\cdot)$ denotes the Landau symbol. Following a similar line of reasoning as in [19, APPENDIX I], \dot{E}_s and \ddot{E}_s are given by

$$\begin{aligned} \dot{E}_s &= \log_2(e) a_s \mathbb{E}(g_s), \\ \ddot{E}_s &= \log_2(e) a_s^2 [\nu \{\mathbb{E}(g_s)\}^2 - (\nu + 1) \mathbb{E}(g_s^2)], \end{aligned} \quad (12)$$

where

$$\begin{aligned} \mathbb{E}(g_s) &= \binom{N_s}{n_s} \left[n_s \Omega_s + \frac{1}{\Omega_s} \sum_{l=1}^{N_s-n_s} (-1)^{n_s+l-1} \binom{N_s-n_s}{l} \right. \\ &\quad \times \left. \left(\frac{n_s}{l} \right)^{n_s-1} \left\{ \Phi_{s,l}^{-2} - \sum_{m=0}^{n_s-2} (m+1) \Omega_s^2 \binom{-l}{n_s}^m \right\} \right], \\ \mathbb{E}(g_s^2) &= \binom{N_s}{n_s} \left[\frac{\Gamma(n_s+2) \Omega_s^{n_s+2}}{\Omega_s^{n_s} (n_s-1)!} + \frac{1}{\Omega_s} \sum_{l=1}^{N_s-n_s} (-1)^{n_s+l-1} \right. \\ &\quad \times \binom{N_s-n_s}{l} \left(\frac{n_s}{l} \right)^{n_s-1} \left\{ 2 \left(\frac{\Omega_s}{\Phi_{s,l}} \right)^3 - \sum_{m=0}^{n_s-2} \frac{1}{m!} \right. \\ &\quad \times \left. \left. \left(\frac{-l}{n_s \Omega_s} \right)^m \Gamma(m+3) \Omega_s^{m+3} \right\} \right]. \end{aligned}$$

The integrals in $\mathbb{E}(g_s)$ and $\mathbb{E}(g_s^2)$ are solved using [17, eqn. (3.351-3), p. 340]. Therefore, a closed-form expression for the low-SNR approximation of E_s can be obtained using (11) and (12). Similarly, for x_w , we have

$$\begin{aligned} \dot{E}_w &= \log_2(e) a_w \mathbb{E}(g_{\min}), \\ \ddot{E}_w &= \log_2(e) a_w \left[\nu a_w \{\mathbb{E}(g_{\min})\}^2 \right. \\ &\quad \left. - \{(\nu + 1) a_w - 2a_s\} \mathbb{E}(g_{\min}^2) \right] \end{aligned} \quad (13)$$

Since it is somewhat tedious to obtain closed-form expressions of $\mathbb{E}(g_{\min})$ and $\mathbb{E}(g_{\min}^2)$, we present closed-form analysis for two special cases.

Case I ($n_s = n_w = n = 1$): In this case, NOMA-GSC reduces to NOMA-SC. Therefore, we have

$$\begin{aligned} \mathbb{E}(g_{\min}) &= \mathbb{E}(g_{\min,SC}) = \int_0^\infty x f_{g_{\min,SC}}(x) dx \\ &= \sum_{k=1}^{N_s} \sum_{j=1}^{N_w} \binom{N_s}{k} \binom{N_w}{j} \frac{(-1)^{k+j}}{\chi_{k,j}}, \\ \mathbb{E}(g_{\min}^2) &= \mathbb{E}(g_{\min,SC}^2) = \int_0^\infty x^2 f_{g_{\min,SC}}(x) dx \\ &= \sum_{k=1}^{N_s} \sum_{j=1}^{N_w} \binom{N_s}{k} \binom{N_w}{j} \frac{2(-1)^{k+j}}{\chi_{k,j}^2}. \end{aligned}$$

Using the two preceding expressions together with (11) and (13), we can obtain a closed-form expression for the low-SNR approximation of E_w for $n_s = n_w = 1$.

Case II: ($n_s = N_s, n_w = N_w$): In this case NOMA-GSC reduces to NOMA-MRC. Therefore,

$$\begin{aligned} \mathbb{E}(g_{\min}) &= \mathbb{E}(g_{\min,MRC}) = \int_0^\infty x f_{g_{\min,MRC}}(x) dx \\ &= \frac{1}{\Gamma(N_s) \Omega_s^{N_s}} \sum_{j=0}^{N_w-1} \frac{(N_s+j)! \chi_{1,1}^{-(N_s+j+1)}}{j! \Omega_w^j} \\ &\quad + \frac{1}{\Gamma(N_w) \Omega_w^{N_w}} \sum_{k=0}^{N_s-1} \frac{(N_w+k)! \chi_{1,1}^{-(N_w+k+1)}}{k! \Omega_s^k}, \\ \mathbb{E}(g_{\min}^2) &= \mathbb{E}(g_{\min,MRC}^2) = \int_0^\infty x^2 f_{g_{\min,MRC}}(x) dx \\ &= \frac{1}{\Gamma(N_s) \Omega_s^{N_s}} \sum_{j=0}^{N_w-1} \frac{(N_s+j+1)! \chi_{1,1}^{-(N_s+j+2)}}{j! \Omega_w^j} \\ &\quad + \frac{1}{\Gamma(N_w) \Omega_w^{N_w}} \sum_{k=0}^{N_s-1} \frac{(N_w+k+1)! \chi_{1,1}^{-(N_w+k+2)}}{k! \Omega_s^k}. \end{aligned}$$

Using the two preceding expressions together with (11) and (13), we can obtain a closed-form expression for the low-SNR approximation of E_w for $n_s = N_s$ and $n_w = N_w$.

E. Upper-bound on the effective capacity of NOMA-GSC

In this subsection, we derive a fundamental upper-bound on the EC of NOMA-GSC, using Jensen's inequality. Using the fact that $-\log_2(\cdot)$ is a *log-concave* function, from (3) it follows that

$$\begin{aligned} E_i &\leq -\frac{1}{\nu} \mathbb{E}_{\gamma_i} [\log_2 \{(1 + \gamma_i)^{-\nu}\}] \\ &= \mathbb{E}_{\gamma_i} [\log_2(1 + \gamma_i)] \triangleq \tilde{E}_i. \end{aligned} \quad (14)$$

It is important to note that \tilde{E}_i is independent of the delay exponent θ and represents the average achievable rate of x_i in NOMA-GSC. This bound is also consistent with the fact that the EC of NOMA-GSC is always less than or equal to the average achievable rate (the equality holds for the case when $\theta \rightarrow 0$). A closed-form expression for an upper-bound on $\tilde{E}_{\text{sum}} = \tilde{E}_s + \tilde{E}_w$, which is very tight in the mid-to-high SNR range can be obtained using [15, eqns. (2), (4)].

IV. RESULTS AND DISCUSSION

In this section, we present the numerical and analytical results for the EC of NOMA-GSC and OMA-GSC. We consider a system where $N_s = N_w = N = 4$, $n_s = n_w = n$, $\Omega_s = 1$, $\Omega_w = 0.1$, $T = 0.01$ ms, $B = 100$ kHz. As reported in [15], the optimal power allocation in a NOMA-GSC system depends on the target data rate of x_i . Considering the target data rate for both x_s and x_w to be 2 bps/Hz, it follows from [15] that a valid range for a_s is given

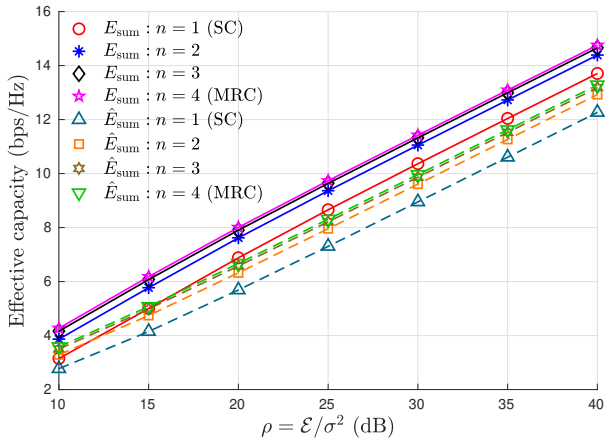


Fig. 1. Comparison of EC for NOMA-GSC and OMA-GSC with $\theta = 1$.

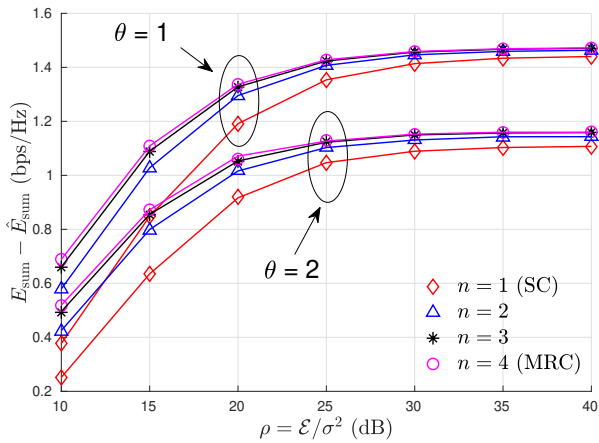


Fig. 2. Difference between the ECs of NOMA-GSC and OMA-GSC.

by $0 < a_s < 0.25$. Note that throughout this section, results for the sum EC are presented for the case where the sum EC is optimized using a one-dimensional search over $a_s \in \{0.1, 0.2, \dots, 0.24\}$. Similarly, results for the achievable sum rate are presented for a similarly optimized value of a_s .

Fig. 1 shows a comparison of EC in NOMA-GSC and OMA-GSC for different values of n . Markers in the figure denote the numerically evaluated results. The dashed lines (without markers) denote the closed-form analytical results for the sum EC of OMA-GSC. For the case of NOMA-GSC, the solid lines (without markers) for $n = 1$ and $n = 4$ denote the closed-form analytical results, whereas the solid lines (without markers) for $n = 2$ and $n = 3$ represent the semi-analytical results where E_s is evaluated using the closed-form expression and E_w is evaluated numerically. An excellent agreement between the numerical and analytical/semi-analytical results confirms the correctness of the analysis. The optimal value of a_s that maximizes the sum EC of NOMA-GSC is found to be 0.24 (the maximum possible value considered in the

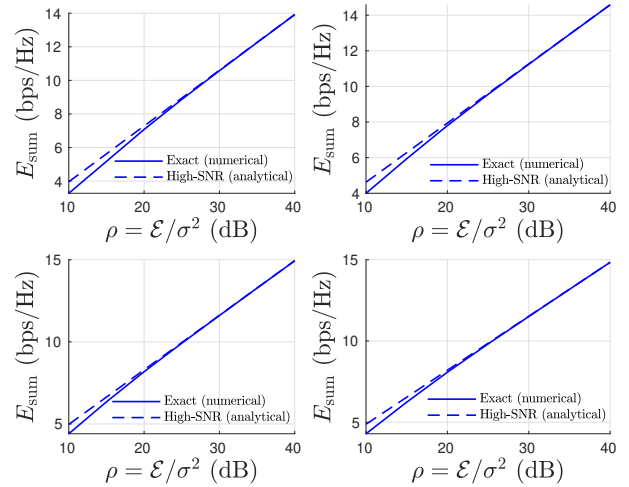


Fig. 3. High-SNR approximation for the sum EC of NOMA-GSC. Clockwise from the top-left: $n = 1$ (SC), 2, 3, 4 (MRC).

range $0 < a_s < 0.24$). This occurs because most of the EC in E_{sum} is obtained by E_s (as x_s is decoded without any inter-symbol interference and the links between S and U_s are comparatively stronger).

It can be noted from the figure that NOMA-GSC outperforms OMA-GSC for any value of n . More interestingly, it can be observed that the gain in the sum EC achieved by moving from n to $n + 1$ combined paths decreases with increasing n . These results are further elaborated in Fig. 2. In the figure, markers denote the numerically evaluated results, whereas the solid lines (without markers) denote the analytical/semi-analytical results. It can be noted from the figure that the difference between E_{sum} and \hat{E}_{sum} increases in the low-to-mid SNR regime, with increasing ρ and also with increasing n . This difference then saturates in the high-SNR range (which is in line with the results in [9]) and most of the gain is obtained by using only two strongest diversity paths. As the value of θ increases, the figure shows a decrease in the performance difference between NOMA and OMA, which means that the performance of NOMA and OMA both degrade severely under a stringent delay requirement.

Figs. 3 and 4 show the high-SNR and low-SNR approximations for the sum EC of NOMA-GSC for $\theta = 0.5$, respectively. An excellent match can be noticed from both the figures between the exact (numerically evaluated) values of E_{sum} and the analytically/semi-analytically evaluated approximations. It can be noted from these figures that there is an exponential growth in the sum EC in the low-SNR regime, and a linear growth in the high-SNR regime.

Fig. 5 shows the effect of the delay QoS constraint θ on the difference between the average achievable sum rate and EC of NOMA-GSC (i.e., $\hat{E}_{\text{sum}} - E_{\text{sum}}$) for different values of n . First, it can be noted from the figure that an increase in the value of θ results in a very severe system perfor-

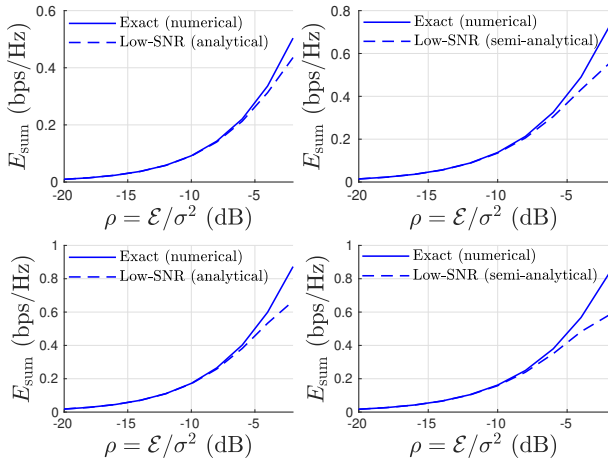


Fig. 4. Low-SNR approximation for the sum EC of NOMA-GSC. Clockwise from the top-left: $n = 1$ (SC), 2, 3, 4 (MRC).

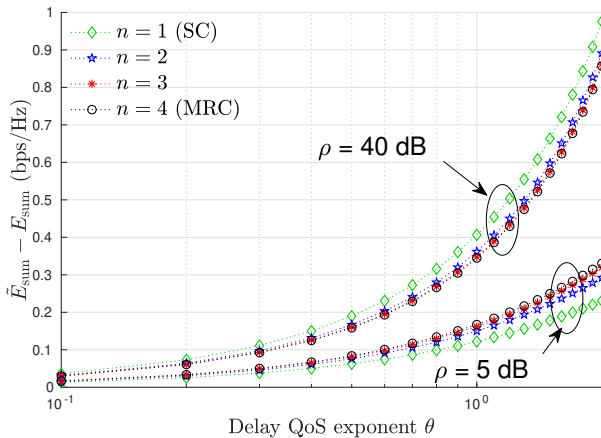


Fig. 5. Difference between average achievable rate and effective capacity for different values of θ and n .

mance degradation as the value of $\hat{E}_{\text{sum}} - E_{\text{sum}}$ grows very rapidly for large θ . This means that a system with strict delay constraints will have a much lower EC as compared to the average achievable rate. Furthermore, it can be noted from the figure that with an increase in the value of ρ , the difference between the average achievable rate and the effective capacity increases. It is also interesting to note that for low values of ρ , although increasing the number of combined paths increases both \hat{E}_{sum} and E_{sum} , the difference between these two quantities also increases. For large values of ρ , by combining more diversity paths at the receiver, the difference between \hat{E}_{sum} and E_{sum} decreases. Therefore, in order to achieve a desired quality of service in terms of delay QoS exponent and data rate, a higher transmit power requirement is needed than that predicted by the traditional achievable rate analysis.

V. CONCLUSION

In this paper, we have presented the effective capacity analysis of a two-user single-input multiple-output down-

link NOMA system with generalized selection combining receivers. We derived closed-form expressions for the sum EC of NOMA-GSC and OMA-GSC. We also presented high and low-SNR approximations for the sum EC of NOMA-GSC. Our results indicate that the sum EC grows exponentially in the low-SNR regime and linearly in the high-SNR regime. The high-SNR analysis of the sum EC confirmed that no benefit is obtained in terms of EC by having multiple antennas at the weak user. The results also indicate that most of the gain in terms of sum EC is obtained by combining the signals received from the strongest diversity paths, while diminishing returns are obtained by increasing the number of combined paths. By quantifying the difference between average achievable sum rate and sum effective capacity, we showed that for a system with stringent delay requirements, the achievable link-layer rate is significantly smaller than the ergodic rate, and this difference increases with an increase in SNR. The presented analysis serves as a practical system design tool which can be efficiently applied to any configuration in order to determine the appropriate number of diversity paths to be combined to achieve a delay-constrained target quality-of-service.

REFERENCES

- [1] Y. Liu, Z. Qin, M. Elkashlan, Z. Ding, A. Nallanathan, and L. Hanzo, "Nonorthogonal multiple access for 5G and beyond," *Proc. of the IEEE*, vol. 105, no. 12, pp. 2347–2381, Dec 2017.
- [2] M. Vaezi, Z. Ding, and H. Poor, *Multiple Access Techniques for 5G Wireless Networks and Beyond*. Springer International Publishing, 2018.
- [3] Z. Ding, M. Peng, and H. V. Poor, "Cooperative non-orthogonal multiple access in 5G systems," *IEEE Commun. Lett.*, vol. 19, no. 8, pp. 1462–1465, Aug 2015.
- [4] J. Men and J. Ge, "Non-orthogonal multiple access for multiple-antenna relaying networks," *IEEE Commun. Lett.*, vol. 19, no. 10, pp. 1686–1689, Oct 2015.
- [5] M. Zeng, A. Yadav, O. A. Dobre, G. I. Tsiropoulos, and H. V. Poor, "On the sum rate of MIMO-NOMA and MIMO-OMA systems," *IEEE Wireless Commun. Lett.*, vol. 6, no. 4, pp. 534–537, Aug 2017.
- [6] Dapeng Wu and R. Negi, "Effective capacity: a wireless link model for support of quality of service," *IEEE Trans. Wireless Commun.*, vol. 2, no. 4, pp. 630–643, July 2003.
- [7] M. Matthaiou, G. C. Alexandropoulos, H. Q. Ngo, and E. G. Larsson, "Analytic framework for the effective rate of MISO fading channels," *IEEE Trans. Commun.*, vol. 60, no. 6, pp. 1741–1751, June 2012.
- [8] S. Chen, J. Zhang, G. K. Karagiannidis, and B. Ai, "Effective rate of MISO systems over Fisher-Snedecor \mathcal{F} fading channels," *IEEE Commun. Lett.*, vol. 22, no. 12, pp. 2619–2622, Dec 2018.
- [9] W. Yu, L. Musavian, and Q. Ni, "Link-layer capacity of NOMA under statistical delay QoS guarantees," *IEEE Trans. Commun.*, vol. 66, no. 10, pp. 4907–4922, Oct 2018.
- [10] J. Choi, "Effective capacity of NOMA and a suboptimal power control policy with delay QoS," *IEEE Trans. Commun.*, vol. 65, no. 4, pp. 1849–1858, April 2017.
- [11] X. Chen, G. Liu, and Z. Ma, "Statistical QoS provisioning for half/full-duplex cooperative non-orthogonal multiple access," in *2017 IEEE 86th Veh. Tech. Conf. (VTC-Fall)*, Sep. 2017, pp. 1–5.
- [12] C. Xiao, J. Zeng, W. Ni, R. P. Liu, X. Su, and J. Wang, "Delay guarantee and effective capacity of downlink NOMA fading channels," *IEEE J. Sel. Topics Signal Proc.*, vol. 13, no. 3, pp. 508–523, June 2019.

- [13] W. Yu, A. Chorti, L. Musavian, H. V. Poor, and Q. Ni, "Effective secrecy rate for a downlink NOMA network," *IEEE Trans. Wireless Commun.*, to appear.
- [14] M. S. Alouini and M. K. Simon, "An MGF-based performance analysis of generalized selection combining over Rayleigh fading channels," *IEEE Trans. Commun.*, vol. 48, no. 3, pp. 401–415, March 2000.
- [15] V. Kumar, B. Cardiff, and M. F. Flanagan, "Performance analysis of NOMA with generalised selection combining receivers," *Electronics Letters*, to appear. [Online]. Available: https://www.researchgate.net/publication/336326352_Performance_analysis_of_NOMA_with_generalized_selection_combining_receivers
- [16] V. S. Adamchik and O. I. Marichev, "The algorithm for calculating integrals of hypergeometric type functions and its realization in REDUCE system," in *Proceedings of the International Symposium on Symbolic and Algebraic Computation*, 1990, pp. 212–224.
- [17] A. Jeffrey and D. Zwillinger, *Table of Integrals, Series, and Products*, 7th ed. Elsevier Science, 2007.
- [18] C. García-Corrales, F. J. Cañete, and J. F. Paris, "Capacity of $\kappa - \mu$ shadowed fading channels," *International Journal of Antennas and Propagation*, vol. 24, 2014.
- [19] C. Zhong, T. Ratnarajah, K. Wong, and M. Alouini, "Effective capacity of correlated MISO channels," in *2011 IEEE Int. Conf. Commun. (ICC)*, June 2011, pp. 1–5.